Some progress in large-eddy simulation using the 3-D vortex particle method

By G. S. Winckelmans

1. Summary of motivation, accomplishments, and future plans

This two-month visit at CTR was devoted to investigating possibilities in LES modeling in the context of the 3-D vortex particle method (=vortex element method, VEM) for unbounded flows. A dedicated code was developed for that purpose. Although $O(N^2)$ and thus slow, it offers the advantage that it can easily be modified to try out many ideas on problems involving up to $N \approx 10^4$ particles. Energy spectrums (which require $O(N^2)$ operations per wavenumber) are also computed. Progress was realized in the following areas: particle redistribution schemes, relaxation schemes to maintain the solenoidal condition on the particle vorticity field, simple LES models and their VEM extension, possible new avenues in LES. Model problems that involve strong interaction between vortex tubes were computed, together with diagnostics: total vorticity, linear and angular impulse, energy and energy spectrum, enstrophy. More work is needed, however, especially regarding relaxation schemes and further validation and development of LES models for VEM. Finally, what works well will eventually have to be incorporated into the fast parallel tree code.

2. The 3-D VEM method

We use the 3-D regularized vortex particle method (=vortex element method, VEM) as in Winckelmans & Leonard (1993). The particle representation of the vorticity field is then taken as

$$\tilde{\omega}_\sigma(\mathbf{x},t) = \sum_s \frac{1}{\sigma^3}\,\zeta\left(\frac{\|\mathbf{x}-\mathbf{x}^s(t)\|}{\sigma}\right)\,\gamma^s(t) \tag{1}$$

with $\gamma^s(t) = \omega^s(t)\,\mathrm{vol}^s$ the particle strength, ζ the regularization function, and σ the core size. All particles have the same core size, and it remains constant in time. Particles usually have the same volume of fluid, vol, associated with them (e.g., $\mathrm{vol} = h^3$ for particles initially on an $h \times h \times h$ lattice). Sometimes however, the discretization of an initial condition (such as a torus for discretizing a vortex ring) leads to particle volumes that are not quite identical, see e.g., Winckelmans & Leonard (1993). Since the flow is incompressible, the particle volume remains constant in time. We also define the singular (delta-function) particle representation of the vorticity field as

$$\tilde{\omega}(\mathbf{x},t) = \sum_s \delta\left(\mathbf{x}-\mathbf{x}^s(t)\right)\,\gamma^s(t)\;. \tag{2}$$

The velocity field, $\mathbf{u}_\sigma$, is computed from the particle representation of the vorticity field as the curl of the vector potential, $\tilde{\psi}_\sigma$, which solves $\nabla^2 \tilde{\psi}_\sigma = -\tilde{\omega}_\sigma$. Hence it is divergence-free.

Vortex elements are convected by the local velocity

$$\frac{d}{dt}\mathbf{x}^q(t) = \mathbf{u}_\sigma(\mathbf{x}^q(t),t) \ , \tag{3}$$

and their strength is subjected to 3-D stretching by the local velocity gradient. The general mixed scheme is obtained as (Winckelmans 1989, Winckelmans & Leonard 1988, 1989, 1993),

$$\frac{d}{dt}\gamma^q(t) = \Big(\alpha\, \nabla \mathbf{u}_\sigma(\mathbf{x}^q(t),t) + (1-\alpha)\, (\nabla \mathbf{u}_\sigma(\mathbf{x}^q(t),t))^T\Big) \cdot \gamma^q(t) \ . \tag{4}$$

Three different cases are: $\alpha = 1$ for the classical scheme, $\alpha = 0$ for the transpose scheme, and $\alpha = 0.5$ for the symmetric scheme.

For the present version of the VEM code, Gaussian smoothing is used (Leonard 1985, Winckelmans 1989, Winckelmans & Leonard 1993):

$$\zeta(\rho) = \left(\frac{1}{2\pi}\right)^{3/2} e^{-\frac{\rho^2}{2}} \ , \tag{5a}$$

$$G(\rho) = \frac{1}{4\pi\,\rho}\,\mathrm{erf}\left(\frac{\rho}{\sqrt{2}}\right) \ , \tag{5b}$$

$$K(\rho) = \frac{1}{\rho^2}\,(G(\rho) - \zeta(\rho)) \ , \tag{5c}$$

$$F(\rho) = \frac{1}{\rho^2}\,(3K(\rho) - \zeta(\rho)) \ , \tag{5d}$$

with ζ the vorticity smoothing function, G the Green's function for the vector potential (= streamfunction), K the Biot-Savart function for the velocity evaluation, F a function used in evaluating the velocity gradient, and $\rho = r/\sigma$ the dimensionless distance. This choice leads to a second order method, provided $0 < h/\sigma \leq 1$.

The error function $\mathrm{erf}(x)$ is computed using e^{-x^2} and Eq. 7.1.26 in Abramowitz and Stegun (1972). For small ρ, Taylor series expansions are used to evaluate G, K, and F. Notice that, in general, switching from $f = f_a$ if $x < x_0$ to $f = f_b$ if $x \geq x_0$ is programmed without an "if" statement by making use of a Heaviside function:

$$f = f_a + (f_b - f_a)\,\frac{1}{2}(1 + \mathrm{sign}(1, x - x_0)) \ . \tag{6}$$

With the particle strength exchange scheme for viscous diffusion (Mas-Gallic 1987, Degond & Mas-Gallic 1989), we have:

$$\frac{d}{dt}\gamma^q(t) = \cdots + \frac{2\nu}{\sigma^2}\sum_s (\mathrm{vol}^q\,\gamma^s(t) - \mathrm{vol}^s\,\gamma^q(t))\,\frac{1}{\sigma^3}\eta\left(\frac{\|\mathbf{x}^s(t) - \mathbf{x}^q(t)\|}{\sigma}\right) \ , \tag{7}$$

where $\eta(\rho) = -\frac{1}{\rho}\frac{d}{d\rho}\zeta(\rho)$. Note that the Gaussian smoothing is the only one for which $\eta(\rho) = \zeta(\rho)$. (It is also the natural kernel for the diffusion equation (Winckelmans & Leonard 1993).) For non-uniform diffusion coefficients (such as in LES), the formulation simply becomes:

$$\frac{d}{dt}\gamma^q(t) = \cdots$$
$$+\frac{1}{\sigma^2}\sum_s \left(\nu(\mathbf{x}^s(t)) + \nu(\mathbf{x}^q(t))\right)\left(\mathrm{vol}^q\,\gamma^s(t) - \mathrm{vol}^s\,\gamma^q(t)\right)\frac{1}{\sigma^3}\eta\left(\frac{\|\mathbf{x}^s(t) - \mathbf{x}^q(t)\|}{\sigma}\right). \tag{8}$$

2.1 Particle redistribution schemes

One needs to maintain the condition that particle cores overlap. In some cases, this calls for a particle redistribution scheme. The high order Λ_2 scheme used by Koumoutsakos (1993) and Koumoutsakos & Leonard (1992, 1995) was adopted. It consists of replacing the whole set of vortex particles by a new set. The new particles are located on an $h \times h \times h$ lattice (hence all particles have vol $= h^3$). Consider first the normalized 1-D problem with unit spacing. Then, in the $\Lambda_2(x)$ scheme, an old particle located at $-\frac{1}{2} \le x \le \frac{1}{2}$ gives $-\frac{1}{2}x(1-x)$ of its strength to the new particle located at -1, $(1-x)(1+x)$ of its strength to the new particle located at 0, and $\frac{1}{2}x(1+x)$ to the new particle located at 1. This scheme is such that:

$$x^n = (-1)^n\left(-\frac{1}{2}x(1-x)\right) + (0)^n\left((1-x)(1+x)\right) + (1)^n\left(\frac{1}{2}x(1+x)\right) \tag{9}$$

for $n = 0, 1, 2$. In 3-D, one applies the scheme as $\Lambda_2(x)\,\Lambda_2(y)\,\Lambda_2(z)$. This scheme then conserves exactly total vorticity, $\mathbf{\Omega} = \int_V \omega\, d\mathbf{x} = \sum_s \gamma^s$, linear impulse, $\mathbf{I} = \frac{1}{2}\int_V \mathbf{x}\times\omega\, d\mathbf{x} = \frac{1}{2}\sum_s \mathbf{x}^s \times \gamma^s$, and angular impulse, $\mathbf{A} = \frac{1}{3}\int_V \mathbf{x}\times(\mathbf{x}\times\omega)\, d\mathbf{x} = \frac{1}{3}\sum_s \mathbf{x}^s \times (\mathbf{x}^s \times \gamma^s)$. It usually performs very well on energy conservation and well on enstrophy conservation.

Notice that a simpler scheme is the Λ_1 scheme: in that case, an old particle located at $-\frac{1}{2} \le x \le \frac{1}{2}$ gives $\frac{1}{2} - x$ of its strength to the new particle located at $-\frac{1}{2}$, and $\frac{1}{2} + x$ to the new particle located at $\frac{1}{2}$. This scheme is such that:

$$x^n = \left(-\frac{1}{2}\right)^n\left(\frac{1}{2} - x\right) + \left(\frac{1}{2}\right)^n\left(\frac{1}{2} + x\right) \tag{10}$$

for $n = 0, 1$. Again, in 3-D, one applies the scheme as $\Lambda_1(x)\,\Lambda_1(y)\,\Lambda_1(z)$. This scheme then conserves exactly total vorticity and linear impulse. It does not conserve angular impulse. It usually performs poorly on energy conservation and very poorly on enstrophy conservation. We do not recommend its use.

The Λ_2 scheme has been incorporated in the fast 3-D parallel tree code as well (Winckelmans *et al.* 1995). Particle redistribution is programmed using the tree code data structure. It runs very efficiently. Its cost is much less than the cost associated with the field evaluation.

2.2 Relaxation schemes for the particle vorticity field

The particle representation of the vorticity field, $\tilde{\omega}_\sigma$, does not constitute a generally divergence-free basis (Saffman & Meiron 1986, Winckelmans & Leonard 1988, 1993). Thus, although the initial particle discretization of a vorticity field can be made very near divergence-free, this condition does not necessarily remain satisfied in long time computations. A relaxation scheme can be applied, if and when necessary, which ensures that the particle field, $\tilde{\omega}_\sigma$, remains a good representation of the true divergence-free vorticity field, $\omega_\sigma = \nabla \times \mathbf{u}_\sigma$. Different approaches have been proposed (Winckelmans 1989, Pedrizzetti 1992, Winckelmans & Leonard 1993).

Notice first that, once computed, the velocity gradient tensor, $\nabla \mathbf{u}_\sigma$, contains all the necessary components to evaluate the true vorticity field at the particle locations. This vorticity field is then used in both relaxation schemes considered here. Notice also that $\omega_\sigma = \nabla \times \mathbf{u}_\sigma = \nabla \times (\nabla \times \tilde{\psi}_\sigma) = -\nabla^2 \tilde{\psi}_\sigma + \nabla(\nabla \cdot \tilde{\psi}_\sigma)$. Recalling that $\nabla^2 \tilde{\psi}_\sigma = -\tilde{\omega}_\sigma$, it follows that $\nabla(\nabla \cdot \tilde{\psi}_\sigma) = \omega_\sigma - \tilde{\omega}_\sigma$.

The P-relaxation scheme (Pedrizzetti 1992) was developed in the framework of singular vortex particles. It is modified to be used in the context of regularized vortex particles. At every time step, the particle strength vector is modified using the filtering:

$$\gamma^q_{\text{new}} = (1 - f\,\Delta t)\,\gamma^q + f\,\Delta t\,\frac{\omega_\sigma(\mathbf{x}^q)}{\|\omega_\sigma(\mathbf{x}^q)\|}\|\gamma^q\| \tag{11}$$

where $\omega_\sigma(\mathbf{x}^q)$ is the true local vorticity field and where f is a frequency factor. The time scale $1/f$ must be "tuned" with respect to the time scale(s) of the physical phenomena under study to give satisfactory results. This relaxation scheme basically acts as a "spring" that tries to maintain the particle strength vector aligned with the true vorticity vector. This simple scheme is such that: (1) It doesn't do anything to the particle strength vector if that vector is aligned with the vorticity vector; (2) It is a simple local operation on the particle strength vector. No system of linear equations involving neighbor particles needs to be solved.

The W-relaxation scheme (Winckelmans 1989, Winckelmans & Leonard 1993) is based on the functional representation of the vorticity field: one requires that, at particle locations, the particle vorticity field be equal to the true vorticity field:

$$\sum_s \frac{1}{\sigma^3}\,\zeta\left(\frac{\|\mathbf{x}^q - \mathbf{x}^s\|}{\sigma}\right)\,\gamma^s_{\text{new}} = \omega_\sigma(\mathbf{x}^q)\ . \tag{12}$$

This scheme is best applied after the particle redistribution scheme . The fact that the particles are then well-aligned on a regular lattice greatly favors the reconstruction of a smooth function from the particle strengths.

It is also best to use Gaussian smoothing as this smoothing permits a "good-quality" reconstruction of a smooth function from the particle strengths in the whole range of core overlapping: $0 < h/\sigma \leq 1.5$. With other smoothings, the window of acceptable h/σ is much narrower.

The W-scheme amounts to solving a system of linear equations involving only near neighbors. This is done using an iterative method such as Relaxed-Jacobi (in

the tree code) or Relaxed Gauss-Seidel. Notice that the matrix is not diagonally dominant. Actually, with Gaussian smoothing and particles on a regular lattice in d-dimension, the diagonal dominance is violated as soon as $\left(\left(\frac{1}{2\pi}\right)^{1/2} \frac{h}{\sigma}\right)^d \leq \frac{1}{2}$: In 1-D, this means $h/\sigma \leq 1.25$. In 2-D, $h/\sigma \leq 1.77$, and in 3-D, $h/\sigma \leq 1.99$. Thus: (1) The higher the dimension, the worse the non-diagonal dominance; (2) The smaller h/σ, the worse the non-diagonal dominance. Since we operate here in 3-D, and at $h/\sigma = 0.75 - 1.0$ or so (to satisfy the core overlapping condition), we definitely do not have diagonal dominance.

At this point, the efficient iterative solution of this system is still a subject of active research (A. Leonard, private communication). There appears to be an "operating window" of h/σ where, although not diagonally dominant, all eigenvalues of the matrix are still real and positive. In that case, iterative solvers (with or without preconditioning) can be developed. For instance, it is known that the Gauss-Seidel iteration converges for any symmetric, positive definite matrix (Golub and Van Loan 1983). The matrix here is symmetric. It is also positive-definite as long as all eigenvalues remain real and positive.

2.3 Time integration

For time integration, the $O\left((\Delta t)^2\right)$ Adams-Bashforth scheme (AB2) is used. Since this scheme is not self-starting, an $O\left((\Delta t)^2\right)$ Runge-Kutta scheme (RK2) is used for the first time step (after the initial condition or after each use of the particle redistribution scheme). This approach allows one to maintain second order accuracy. Numerical experiments have indeed shown that an $O(\Delta t)$ Euler scheme for the start-up step is simply not acceptable. The RK2 scheme is efficiently programmed as follows: Euler predictor, Trapezoidal-rule corrector.

3. Energy, enstrophy, and their spectrum

A formulation developed by Leonard (1976 unpublished, private communication) (see also Leonard 1985, Shariff *et al.* 1989), is used to compute the energy spectrum. Although developed in the context of vortex filament methods (for which the filament vorticity field is, by construction, equal to the true vorticity field), the formulation also applies to vortex particle methods as long as the particle vorticity field, $\tilde{\omega}_\sigma$, remains a good representation of the true vorticity field, ω_σ. If this condition is violated, then the evaluation of the energy and of its spectrum becomes very complex, see e.g., Winckelmans (1989), Winckelmans & Leonard (1993), Kiya (1993).

With Gaussian smoothing, the energy spectrum is finally obtained as

$$E(k) = e^{-\frac{(k\sigma)^2}{2}}\, \hat{E}(k) \quad \text{with} \quad \hat{E}(k) = \left(\frac{1}{2\pi}\right)^2 \sum_q \sum_s \frac{\sin\left(k\|\mathbf{x}^q - \mathbf{x}^s\|\right)}{k\|\mathbf{x}^q - \mathbf{x}^s\|}\, \gamma^q \cdot \gamma^s \;, \tag{13}$$

and the total energy as (Winckelmans & Leonard 1993)

$$E = \int_0^\infty E(k)\, dk = \frac{1}{2} \sum_q \sum_s \frac{1}{4\pi\|\mathbf{x}^q - \mathbf{x}^s\|} \operatorname{erf}\left(\frac{\|\mathbf{x}^q - \mathbf{x}^s\|}{\sqrt{2}\,\sigma}\right) \gamma^q \cdot \gamma^s$$

$$= \frac{1}{2} \int_V \tilde{\psi}_\sigma \cdot \tilde{\omega}\, d\mathbf{x} = \frac{1}{2} \int_V \tilde{\psi}_{\frac{\sigma}{\sqrt{2}}} \cdot \tilde{\omega}_{\frac{\sigma}{\sqrt{2}}}\, d\mathbf{x} \,. \tag{14}$$

The enstrophy spectrum is $\mathcal{E}(k) = k^2\, E(k)$ and the total enstrophy is (Winckelmans & Leonard 1993)

$$\begin{aligned}
\mathcal{E} &= \int_0^\infty k^2\, E(k)\, dk = \frac{1}{2} \sum_q \sum_s \left(\frac{1}{2\pi}\right)^{3/2} \frac{1}{\sigma^3} \exp\left(-\frac{\|\mathbf{x}^q - \mathbf{x}^s\|^2}{2\,\sigma^2}\right) \gamma^q \cdot \gamma^s \\
&= \frac{1}{2} \int_V \tilde{\omega}_\sigma \cdot \tilde{\omega}\, d\mathbf{x} = \frac{1}{2} \int_V \tilde{\omega}_{\frac{\sigma}{\sqrt{2}}} \cdot \tilde{\omega}_{\frac{\sigma}{\sqrt{2}}}\, d\mathbf{x} \,.
\end{aligned} \tag{15}$$

Notice that the cost associated with evaluating the energy spectrum is $O(N^2)$ for each k.

A special case is the vortex ring of circulation Γ and radius R (Leonard 1985). In that case we obtain for the energy spectrum of the infinitely thin vortex ring:

$$\begin{aligned}
\hat{E}(k) &= \left(\frac{1}{2\pi}\right)^2 2\pi\,(\Gamma R)^2 \int_{-\pi}^{\pi} \frac{\sin\left(2kR\left|\sin\frac{\phi}{2}\right|\right)}{2kR\left|\sin\frac{\phi}{2}\right|} \cos\phi\, d\phi \\
&= \left(\frac{1}{2\pi}\right)^2 4\pi\,(\Gamma R)^2 \int_0^{\pi} \frac{\sin\left(2kR\sin\frac{\phi}{2}\right)}{2kR\sin\frac{\phi}{2}} \cos\phi\, d\phi \\
&= \left(\frac{1}{2\pi}\right)^2 4\pi\,(\Gamma R)^2 \frac{1}{kR} \left[\int_0^1 \sin(2kR\mu) \frac{\left(1-\mu^2\right)^{1/2}}{\mu} d\mu \right. \\
&\qquad\qquad \left. - \int_0^1 \sin(2kR\mu) \frac{\mu}{\left(1-\mu^2\right)^{1/2}} d\mu \right] \\
&= \left(\frac{1}{2\pi}\right)^2 4\pi\,(\Gamma R)^2 \frac{\pi}{2} \left[\left(1 + \sum_{n=1}^{\infty} \frac{1}{(2n+1)} \frac{\left(-(kR)^2\right)^n}{(n+1)!\,n!}\right) - \frac{J_1(2kR)}{kR}\right] \\
&= -\,(\Gamma R)^2 \sum_{n=1}^{\infty} \frac{n}{(2n+1)} \frac{\left(-(kR)^2\right)^n}{(n+1)!\,n!} \,.
\end{aligned} \tag{16}$$

This complements a result presented in Leonard (1985):

$$\hat{E}(k) = (\Gamma R)^2 \frac{1}{2} \int_1^1 J_1^2 \left(kR\left(1-\mu^2\right)^{1/2}\right) d\mu \,. \tag{17}$$

The spectrum, computed using a particle discretization of the vortex ring, is presented in Fig. 1. For small kR, $\hat{E}(k) = \frac{(kR)^2}{6}$. For large kR, $\hat{E}(k)$ asymptotes to $\frac{(kR)^{-1}}{2}$ (Leonard 1985). The fact that $\hat{E} \sim (kR)^2$ for small kR is a consequence of the non-zero linear impulse associated with the vortex ring, e.g., see Phillips (1956).

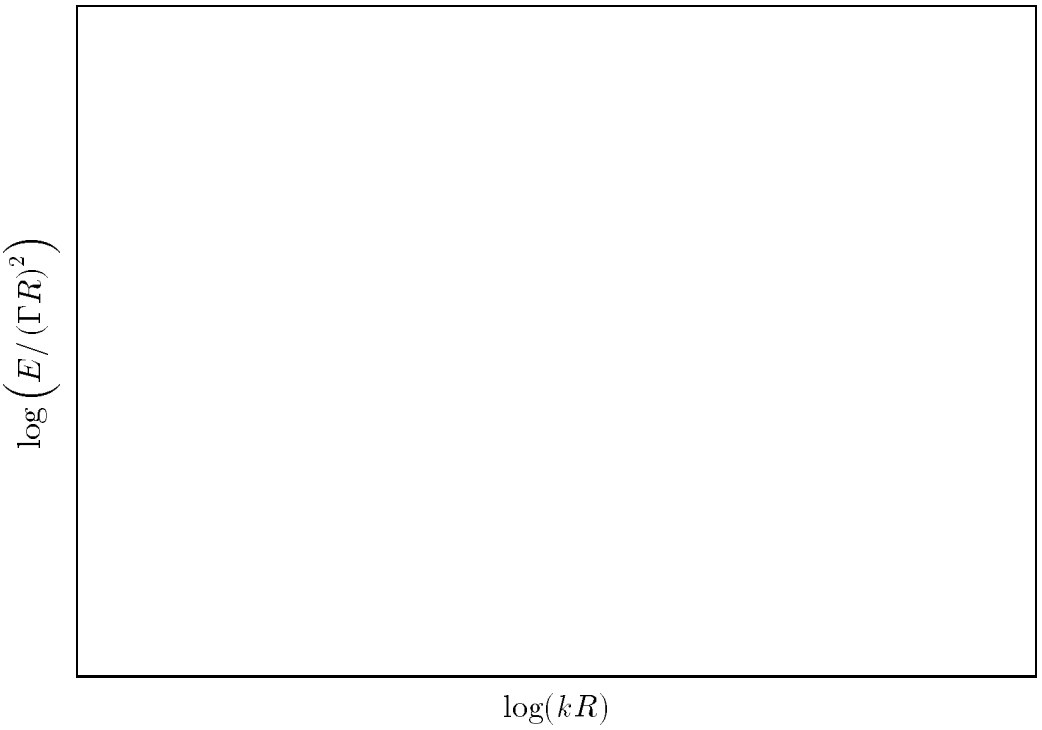

FIGURE 1. Energy spectrum of a singular vortex ring: ——— ; $(kR)^2/6$: - - - - ; $(kR)^{-1}/2$: ····· .

It is found numerically that for a given wavenumber, k, the spacing, h, between the particles used to discretize a ring only needs to satisfy $kh \leq 5$ or so in order for the discrete sum, Eq. (13), to correctly capture the exact integral, Eq. (16). This is very surprising (and not understood at this time) because the integrand varies quite a bit from one particle to the next (1 versus roughly $\frac{\sin(kh)}{kh}$).

For comparison with the single vortex ring, the spectrum of two opposite rings is shown in Fig. 2.

In that case, the linear impulse is zero and one finds that $\hat{E} \sim (kR)^4$. Actually, with sufficient symmetry, one can even create a system with $\hat{E} \sim (kR)^8$. This was obtained by considering six vortex rings on the surface of a cube, see Fig. 3. Finally, we find that all vortex loop configurations considered lead to a spectrum $\hat{E}(k) \sim k^{-1}$ for large k and that this appears to remain so when they evolve in time using VEM, inviscid or viscous (including LES), see Section 5.

4. LES and the possible extension to vortex methods

We consider turbulent flows away from solid boundaries. We also consider the general vorticity formulation (Winckelmans 1989, Winckelmans & Leonard 1993), together with an LES formulation which conserves the zero vorticity divergence (Mansour *et al.* 1978):

$$\frac{D}{Dt}\omega_i = \left(\alpha\frac{\partial u_i}{\partial x_j} + (1-\alpha)\frac{\partial u_j}{\partial x_i}\right)\omega_j + \frac{\partial}{\partial x_j}\left(\nu_{\text{turb}}\left(\frac{\partial \omega_i}{\partial x_j} - \frac{\partial \omega_j}{\partial x_i}\right)\right) \qquad (18)$$

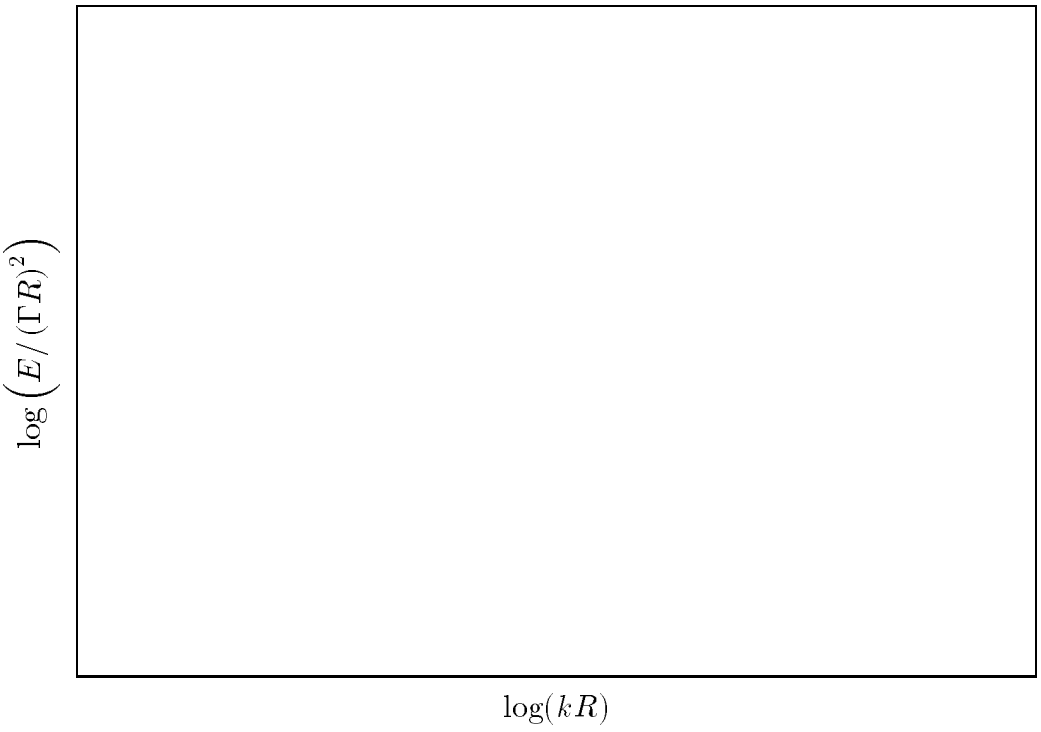

FIGURE 2. Energy spectrum of two opposite singular vortex rings with spacing $S/R = 1.25$: ——— ; $(kR)^4$: - - - - ; $(kR)^{-1}$: ····· .

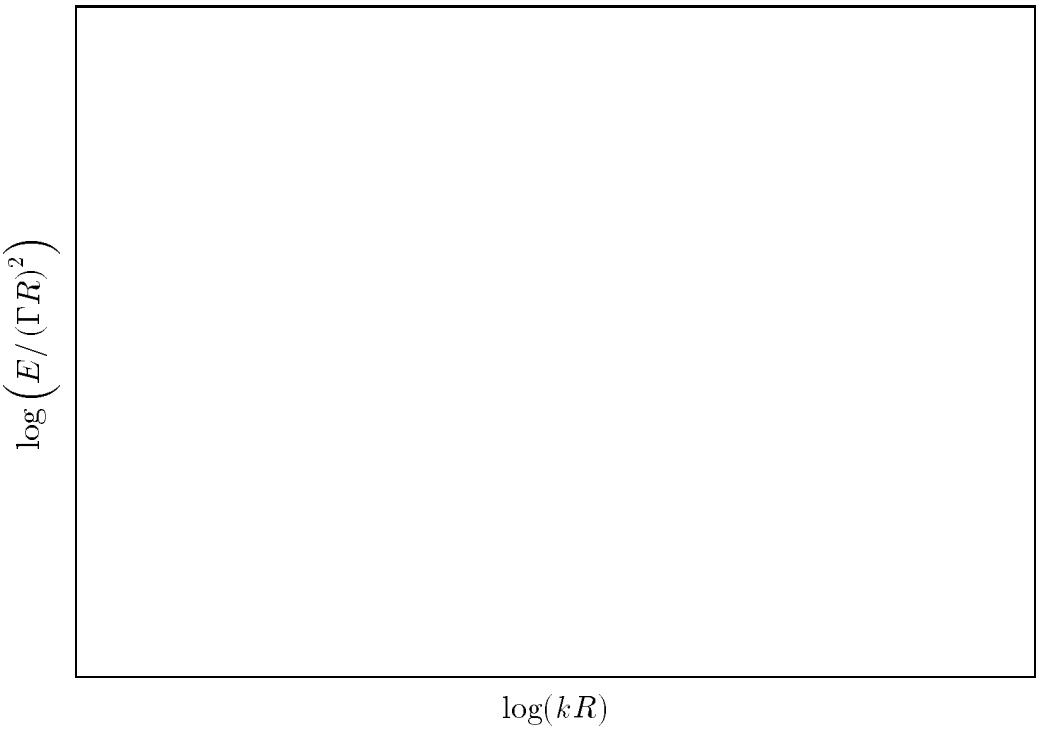

FIGURE 3. Energy spectrum of six singular vortex rings on the surface of a cube of size $S/R = 1.25$: ——— ; $(kR)^8$: - - - - ; $(kR)^{-1}$: ····· .

for any α. The symmetric case $\alpha = 1/2$ leads to $S_{ij}\omega_j$ for the 3-D stretching, with S_{ij} the rate-of-strain tensor.

In the basic LES Smagorinsky's model, the turbulence eddy-viscosity is taken as

$$\nu_{\text{turb}} = (C_s\, h)^2\ (2\, S_{ij}S_{ij})^{1/2} \tag{19}$$

with $S_{ij}S_{ij} = S^2 \geq 0$. Typically, C_s lies in the range $0.1 - 0.24$ (Rogallo & Moin 1984, Lesieur *et al.* 1995). Consider the eigenvalues λ_1, λ_2, and λ_3 of the rate-of-strain tensor, with $\lambda_1 + \lambda_2 + \lambda_3 = S_{ii} = \nabla \cdot \mathbf{u} = 0$. The model then produces an eddy-viscosity

$$\nu_{\text{turb}} = (C_s\, h)^2\ \left(2\left(\lambda_1^2 + \lambda_2^2 + \lambda_3^2\right)\right)^{1/2}\ . \tag{20}$$

We certainly agree with Lesieur *et al.* (1995) that "this simple eddy-viscosity hypothesis is extremely arbitrary, and substantial progress in LES might be achieved by relaxing this assumption". For the time being, however, a simple extension to particle methods of this eddy-viscosity LES model is considered. Since our σ-regularization of the vortex particle method is basically a Gaussian filter, it appears natural to replace the usual Eulerian grid filter h by the particle core size σ (Recall that $h/\sigma = O(1)$) and to take:

$$\nu_{\text{turb}} = (C_s\, \sigma)^2\ (2\, S_{ij}S_{ij})^{1/2}\ . \tag{21}$$

Other simple ways of constructing an LES eddy-viscosity have been proposed, e.g., the model based on local enstrophy of Mansour *et al.* (1978):

$$\nu_{\text{turb}} = (C_v\, h)^2\ (\omega_i\omega_i)^{\frac{1}{2}} \tag{22}$$

with $\omega_i\omega_i = \omega^2 \geq 0$ and $C_v \approx C_s$ ($C_v \approx 0.2$ in Mansour *et al.* 1978). If we recall the vector identity,

$$S^2 = \frac{1}{2}\omega^2 + \nabla \cdot (\nabla \cdot (\mathbf{u}\,\mathbf{u})) \tag{23}$$

together with the Euler equations,

$$\frac{\partial \mathbf{u}}{\partial t} + \nabla \cdot (\mathbf{u}\,\mathbf{u}) \approx -\nabla P\ , \tag{24}$$

it appears that, to first order, the two models differ by $\frac{1}{2}\omega^2 - S^2 \approx \nabla^2 P$. This is an interesting result as it could be used to explain the differences in the behavior of these two models depending on the pressure's Laplacian. Indeed, although $\frac{1}{2}\omega^2$ and S^2 are both positive-definite, their difference, $\nabla^2 P$, can have any sign.

A third model based on the relative rate of change of local enstrophy due to 3-D stretching of vortex lines,

$$\frac{1}{\omega_i\omega_i}\frac{D}{Dt}\left(\omega_i\omega_i\right) = 2\frac{\omega_i S_{ij}\omega_j}{\omega_i\omega_i}\ , \tag{25}$$

could also be constructed, e.g.,

$$\nu_{\text{turb}} = (C_w\, h)^2\ 2\frac{\omega_i S_{ij} \omega_j}{\omega_i \omega_i} \tag{26}$$

This model has the property that it "selects" the eigenvalues used to compute the eddy-viscosity according to the relative orientation between the vorticity vector, ω, and the principal axes (eigen vectors) of the rate-of-strain tensor. Indeed, writing the components of the vorticity vector in the system of principal axes as $(\omega_1, \omega_2, \omega_3)$, this model becomes

$$\nu_{\text{turb}} = (C_w\, h)^2\ 2\left(\frac{\lambda_1 \omega_1^2 + \lambda_2 \omega_2^2 + \lambda_3 \omega_3^2}{\omega_1^2 + \omega_2^2 + \omega_3^2}\right). \tag{27}$$

Hence a vorticity-weighted average of the eigenvalues is used to produce the eddy-viscosity. This model produces a negative eddy-viscosity in regions where enstrophy is decreasing (i.e., where vorticity is compressed). Since this is undesirable, one should use $|\omega_i S_{ij} \omega_j|$ (version 1) or $\max(0, \omega_i S_{ij} \omega_j)$ (version 2) instead of $\omega_i S_{ij} \omega_j$ (version 0).

In axisymmetric strain ($\lambda_1 = \lambda_2 = -\lambda/2$ and $\lambda_3 = \lambda$), the classical LES model gives $(C_s\, h)^2\ \sqrt{3}\,|\lambda|$, regardless of the orientation of the vorticity vector. If vorticity is aligned with the direction of highest rate-of-strain, the "selective" model (version 1) gives $(C_w\, h)^2\ 2\,|\lambda|$. If vorticity is perpendicular to that direction, it gives $(C_w\, h)^2\ |\lambda|$. Since $1 \leq \sqrt{3} \leq 2$, this result also suggests that using $C_w = C_s$ as a first "calibration" for the selective model is a fairly good choice.

In DNS of the Euler equations, the emergence of flat pancake-like structures ("potato chips") that shrink exponentially in time is also observed, e.g., Brachet *et al.* (1992). In that case, two eigenvalues become exponentially large, $\lambda_1 \approx \lambda\left(-\frac{1}{2} - e^{t/T}\right)$, $\lambda_3 \approx \lambda\left(-\frac{1}{2} + e^{t/T}\right)$, while the intermediate eigenvalue, $\lambda_2 \approx \lambda$, remains roughly constant. During this self-similar collapse, it is observed that the vorticity tends to remain aligned with the eigenvector corresponding to the intermediate eigenvalue. Instabilities similar to those leading to streamwise vortices in the context of free shear layers are expected to subsequently concentrate the vorticity and produce isolated vortex filaments. Modeling such flows with LES, a classical model would produce, during the collapse phase, an exponentially large eddy-viscosity (hence kill the collapse phase in its early stages by dissipating the energy rapidly) while the selective model would produce a fairly constant eddy-viscosity (hence dissipate the energy at the end of the collapse phase). Thus, the two models would behave quite differently.

Finally, mixed-schemes that are a judicious combination of the above models could also be considered. Whatever the choice, they would have to be validated somehow (e.g., using DNS data), including the determination of the "constants".

One interesting question is whether one of the simple models above (or a suitable mix of them) can produce better results than what is so far obtained with the classical Smagorinsky's model.

Note that the vortex method also has potential for the development of a dynamic LES model, in the same spirit as in Germano *et al.* (1991), Ghosal *et al.* (1992), Moin & Jiminez (1993), Ghosal & Moin (1994), Moin *et al.* (1994), Ghosal *et al.* (1995). For instance, one could compute the velocity fields and derivatives from the particle locations and strengths by using Gaussian smoothing at two levels: e.g., a filter of width σ and a filter of width $2\,\sigma$. This information could then be used to "compute" C_s in a way similar to what is done so far with dynamic LES in grid methods. One must recall, however, that the vortex method with Gaussian smoothing is a second-order method. If dynamic LES requires higher order methods (as it may . . . , Ghosal, private communication), it might not be feasible in the context of VEM.

5. Fast and slow VEM codes

A fast parallel oct-tree code, originally developed for three-dimensional N-body gravitational problems (Salmon 1990, Salmon & Warren 1994, Warren & Salmon 1995) has been modified into a fast N-vortex code for vortex flow computations using the vortex particle method combined with the particle strength exchange scheme for viscous diffusion, with the Λ_2 particle redistribution scheme, and with both P- and W-relaxation schemes (Salmon, Warren & Winckelmans 1994, Winckelmans *et al.* 1995a,b,c,d).

Gravitation, VEM, etc. are all $O(N^2)$ in complexity: for each of the N elements, find the derivatives of the field induced by all N elements. This is the expensive part of the computation. The other tasks (particle strength exchange scheme, particle redistribution, etc.) are all fairly local operations and are not computationally expensive. The use of fast tree codes in 2-D and 3-D reduces the computing cost associated with all evaluations from $O(N^2)$ to something much more tractable: $O(N \log N)$, or $O(N^{1+\epsilon})$ with $\epsilon << 1$, or even $O(N)$, depending on the complexity of the implementation. The "big-O" notation can, however, be misleading for practical values of N and desired level of accuracy. In our implementations of the VEM, multipole expansions of order $p = 2$ are used (i.e., monopole + dipole + quadrupole). Particular attention is given to ensuring that the error introduced by the use of multipole expansion approximations remains below a desired level for all evaluations. A run-time parameter, $\epsilon_{\rm tol}$, determines the maximum allowed error bound for any particular multipole evaluation.

The tree code is written entirely in ANSI C and has been ported to several parallel and sequential platforms. Problems with $N = O(10^4 - 10^6)$ and beyond are computed on parallel supercomputers. Problems with $N = O(10^3 - 10^5)$ are also computed on the "degenerate" parallel case of single processor workstations.

For the present two-month "exploratory" work at CTR, it was decided to stick with a slow $O(N^2)$ VEM code. (Actually, an all-new VEM code was written for that purpose.) Recall that computing an energy spectrum is also an $O(N^2)$ operation for each wavenumber k anyway. Although this $O(N^2)$ code sets a limit of $N \approx 10^4$ on the number of particles (even on a CRAY C90), it provides for an easy and convenient way of experimenting with many ideas: different LES models, different particle redistribution schemes, different relaxation schemes, etc.

6. Some computational results

6.1 Twelve rings compact vortex system

We consider a "compact" vortex system which, by construction, has the following desirable properties: zero vorticity (as always in 3-D), zero linear impulse, zero angular impulse, and zero helicity, $H = \frac{1}{2}\int_V \mathbf{u}_\sigma \times \tilde{\omega}\, d\mathbf{x}$. Initially, it is formed of twelve circular vortex rings, each of circulation $\Gamma = 1$: six rings of radius $R = 0.6$ (38 sections per ring, with 9 particles per section (1 in the center with circulation $\Gamma/2$, and 8 around the center, at a distance $r_c = 0.123$ and with circulation $\Gamma/16$) laid on the surface of an outer cube of size $S = 1$ and with self-induced velocity directing them towards the cube's center, and six rings of radius $R = 0.3$ (19 sections per ring, again with 9 particles per section) laid on the surface of an inner cube of size $S = 0.5$ and with self-induced velocity directing them away from the cube's center. The total number of particles is $N = 3078$. The spacing between particles along the ring is $h \approx 0.10$. The two cubes share the same center. The outer cube is directed along $\hat{\mathbf{e}}_x = (1,0,0)$, $\hat{\mathbf{e}}_y = (0,0,1)$ and $\hat{\mathbf{e}}_z = \mathbf{e}_x \times \mathbf{e}_y$. To break the symmetry, the inner cube is arbitrarily oriented along $\hat{\mathbf{e}}_x$, $\hat{\mathbf{e}}_y$, $\hat{\mathbf{e}}_z$, with $\hat{\mathbf{e}}_x = \left(\frac{1}{2}, \frac{\sqrt{3}}{4}, -\frac{3}{4}\right)$, $\hat{\mathbf{e}}'_y = \left(0, \frac{\sqrt{3}}{2}, \frac{1}{2}\right)$, $\mathbf{e}_z = \hat{\mathbf{e}}_x \times \hat{\mathbf{e}}'_y$, $\hat{\mathbf{e}}_z = \mathbf{e}_z/\|\mathbf{e}_z\|$ and $\hat{\mathbf{e}}_y = \hat{\mathbf{e}}_z \times \hat{\mathbf{e}}_x$.

To ensure core overlapping for a long time, a large value of $\sigma = 0.20$ is used (hence $h/\sigma \approx 0.5$). The time step is $\Delta t = 0.02$. The symmetric stretching scheme is used, $\alpha = 0.5$. The LES model of Eq. (21) is used, with $C_s = 0.1$. The W-relaxation scheme is used every 10 time steps (with 50 Gauss-Seidel iterations).

Initially, the energy is $E = 1.428$ and the enstrophy $\mathcal{E} = 46.21$. Following classical definition of (isotropic) turbulence, the integral length scale is obtained as

$$L = \frac{3\pi}{4}\frac{\int_0^\infty k^{-1}E(k)\,dk}{E} = 0.490 \tag{28}$$

and the Taylor microscale as

$$\lambda = \left(5\frac{E}{\mathcal{E}}\right)^{1/2} = 0.393\ . \tag{29}$$

At first, a run without particle redistribution is conducted up to $t = 4$. Contour plots are presented in Fig. 4. The histograms of energy and enstrophy are provided in Fig. 5.

The energy decays due to LES diffusion. Due to vortex stretching, the enstrophy first increases. It then decreases due to vortex reconnection by viscous diffusion. Notice that two enstrophy curves are presented. The $\mathcal{E}$-curve refers to enstrophy as defined by Eq. (15). The $\mathcal{E}_b$-curve refers to enstrophy defined as

$$\mathcal{E}_b = \frac{1}{2}\int_V \omega_\sigma \cdot \tilde{\omega}\, d\mathbf{x}\ . \tag{30}$$

As long as the particle vorticity field, $\tilde{\omega}_\sigma$, remains a good representation of the divergence-free field, ω_σ, the two curves remain identical. Their difference is thus a

FIGURE 4. Twelve rings interaction. 3-D contour plots of $\omega_\sigma = 2.0$ at $t = 0.0$ and 2.0 .

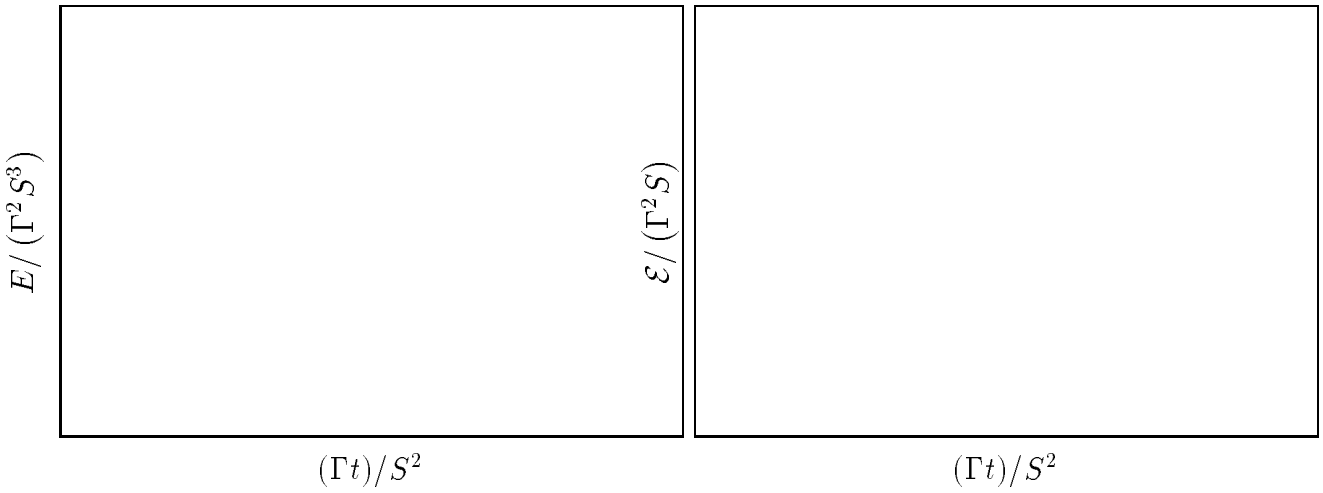

FIGURE 5. Twelve rings interaction. ——— : without redistribution: E and $\mathcal{E}$: • , $\mathcal{E}_b$: × ; ····· : with Λ_1 redistribution: E and $\mathcal{E}$: ▲ (inverted), $\mathcal{E}_b$: × .

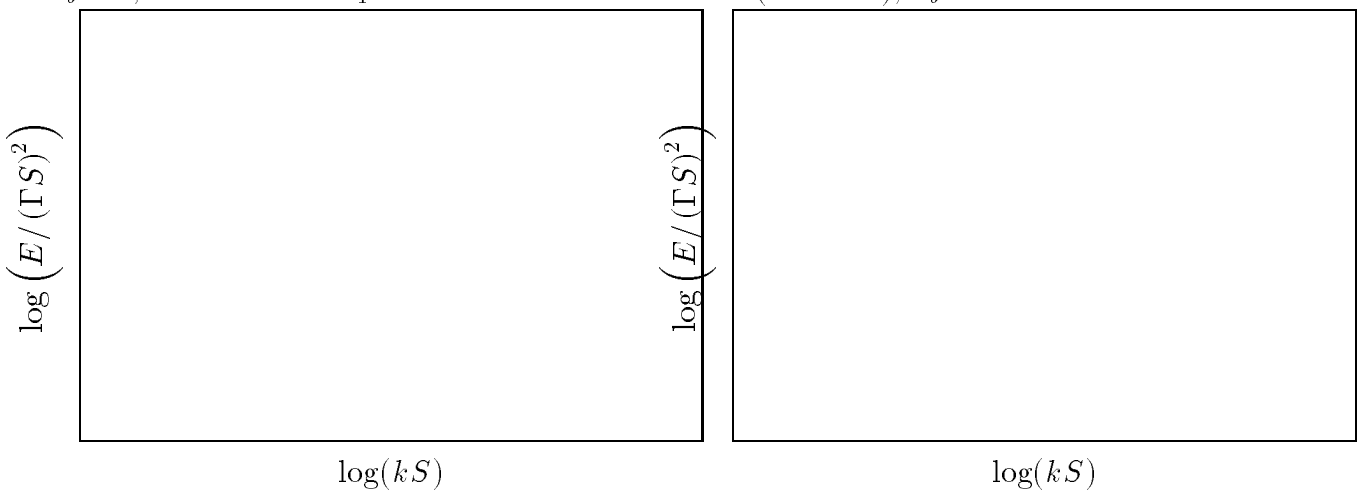

FIGURE 6. Twelve rings interaction. Energy spectrums: $t = 0$: ——— , $t = 1$: – – – – , $t = 2$: ····· , $t = 3$: —·— , $t = 4$: ——— ; k^8, k^6, k^4, k^2, k^{-1}, $k^{-5/3}$: ——— .

global indication of problems with $\tilde{\omega}_\sigma \neq \omega_\sigma$. In the present case, it is seen that the W-relaxation scheme does a fairly good job at keeping $\tilde{\omega}_\sigma \approx \omega_\sigma$ up to $t \approx 2$ or so.

Energy spectrums are provided in Fig. 6. It is seen that the high end of the spectrum starts filling up at $t \approx 2$ or so. This is also indicative of problems with $\tilde{\omega}_\sigma \neq \omega_\sigma$. This is confirmed by a close look, for all particles, at the amplitude of $\tilde{\omega}_\sigma$ and ω_σ and at their relative orientation. It is also seen that the low end of the spectrum does not remain well-behaved as time evolves. The behavior is physically acceptable as long as it remains above $(kS)^4$. The fact that it evolves to $(kS)^2$ indicates that spurious creation of linear impulse has occurred. This is confirmed by a close look at the histogram of $\mathbf{I}(t)$. Finally, total vorticity, $\mathbf{\Omega}(t)$, also does not remain zero as it should. This could be somewhat improved by using the transpose scheme, $\alpha = 0$, instead of the symmetric scheme (Winckelmans 1989, Winckelmans

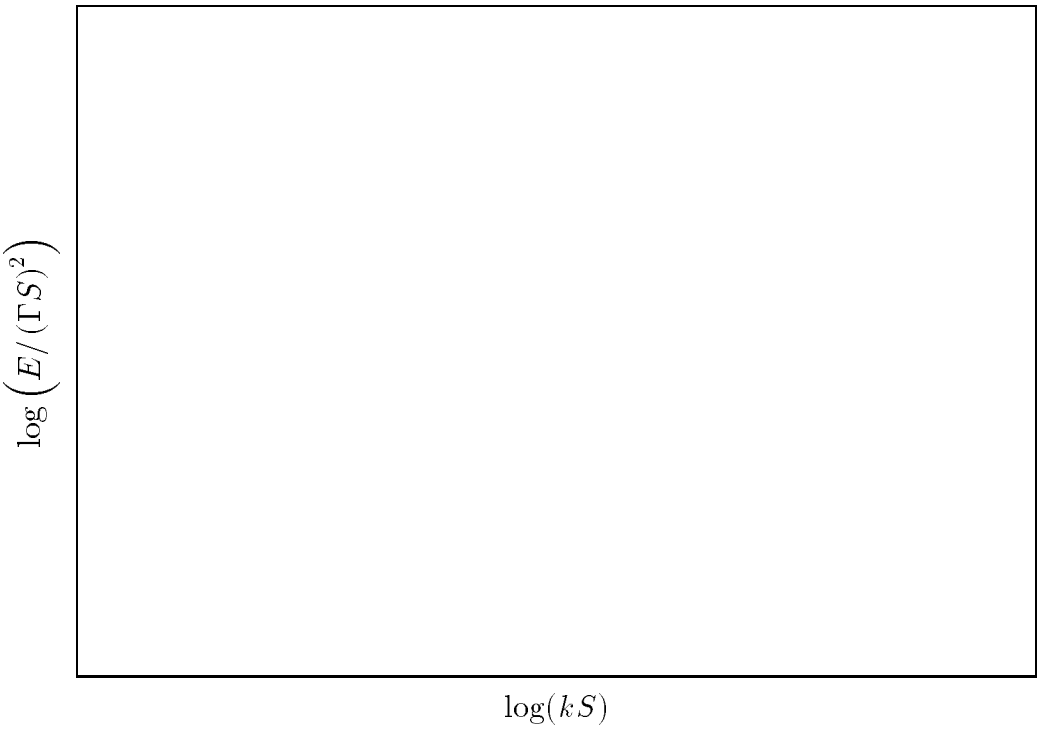

FIGURE 7. Twelve rings interaction. Unfiltered energy spectrums: $t = 0$: ——— , $t = 1$: - - - - , $t = 2$: ····· , $t = 3$: —·— , $t = 4$: — — — ; k^8, k^6, k^4, k^2, k^{-1}: ——— .

& Leonard 1993). The W-relaxation scheme, however, does not conserve $\mathbf{\Omega}$. Again, all the above "symptoms" are indicative of problems with $\tilde{\omega}_\sigma \neq \omega_\sigma$.

For comparison, a run with Λ_1 particle redistribution every 50 time steps (and with $h = 0.10$) is also carried out. From $N = 3078$ at $t = 0$, this leads to $N = 6590$ at $t = 1$, and to $N = 11160$ at $t = 2$. Because of the $O(N^2)$ code, the computation cannot be carried out much further than $t = 2$, and is ended at $t = 2.6$. Histograms of energy and enstrophy are provided in Fig. 5. The conclusion is that the Λ_1 scheme is definitely not acceptable: it dissipates too much energy and enstrophy. In particular, it totally overshadows the amount of energy dissipated by the LES model. Another interesting result is that the correspondence $\tilde{\omega}_\sigma = \omega_\sigma$ is better maintained with particle redistribution than without. This confirms that the W-scheme is indeed best applied when combined with redistribution. Energy spectrums are also provided in Fig. 6. This time, the high end of the spectrum is still fine at $t = 2$. So far, the low end of the spectrum also behaves fine. Although the Λ_1 scheme exactly conserves $\mathbf{\Omega}$ and $\mathbf{I}$, it is likely that spurious creation of $\mathbf{\Omega}$ and $\mathbf{I}$ will also occur eventually due to the W-relaxation scheme and to the symmetric stretching scheme.

One conclusion so far is the following: If one is to do controlled LES with the VEM, it must be that the energy dissipation due to redistribution or relaxation is less than the one due to LES. A good run might be to use the Λ_2 scheme every 10 or 20 steps. (This scheme indeed conserves much better energy and enstrophy, see

below.) This could not be done with the present $O(N^2)$ code, however, due to the large increase in the number of particles required.

Another conclusion is that the W-scheme does not conserve $\mathbf{\Omega}$ and $\mathbf{I}$. (Neither does the P-scheme.) One further improvement would be to develop a relaxation scheme which conserves $\mathbf{\Omega}$ (and, if possible, also conserves $\mathbf{I}$).

One question arises regarding the "inertial" range of such vortex tubes interactions. Is there a $(kS)^{-5/3}$ Kolmogorov range that develops? In Kiya (1993), it is argued that yes, there is. We claim that no, there is not. In considering the filtered energy spectrum, $E(kS)$, of Fig. 6, it is hard to tell whether there is a Kolmogorov range or not. One finds the answer by considering instead the unfiltered energy spectrum, $\hat{E}(kS)$, of Fig. 7. Then, there is a clear indication that (1) the computation blows up (see comments above), and (2) as long as it doesn't blow up, the spectrum remains as $(kS)^{-1}$. This point will become clearer below, on a computation that replicates the one presented in Kiya.

6.2 Six rings compact vortex system

We consider next another compact vortex system with zero vorticity, zero linear impulse, zero angular impulse, and zero helicity. Initially, it is formed of six vortex rings, each of circulation $\Gamma = 1$ and of radius $R = 0.6$ (38 sections per ring, with 9 particles per section (1 in the center with circulation $\Gamma/2$, and 8 around the center, at a distance $r_c = 0.123$ and with circulation $\Gamma/16$) laid on the surface of an outer cube of size $S = 1$ and with self-induced velocity directing them towards the cube's center. The rings are elliptical (in order to break the symmetry) with $ab = R^2$ and $a/b = 1.25$ (top), 0.80 (left), 1.33 (bottom), 0.75 (right), 0.85 (front) and 0.90 (back). The total number of particles is $N = 2052$. The spacing between particles along the ring is $h \approx 0.10$.

A value of $\sigma = 0.14142 \approx \sqrt{2}h$ is used (hence $h/\sigma \approx 0.707$). The time step is $\Delta t = 0.025$ and the computations are carried out up to $t = 4$. The symmetric scheme is used, $\alpha = 0.5$. The LES model of Eq. (21) is used, with $C_s = 0.2$. The W-relaxation scheme is used every 10 time steps (with 50 Gauss-Seidel iterations).

Initially, the energy is $E = 1.745$ and the enstrophy $\mathcal{E} = 65.39$ (hence $\lambda = 0.365$). Notice that the application of the Λ_1 scheme to that perfectly fine initial condition leads to $E = 1.642$ (loss of 6%) and $\mathcal{E} = 57.91$ (loss of 11%) . For comparison the application of the Λ_2 scheme leads to $E = 1.741$ (loss of 0.24%) and $\mathcal{E} = 64.84$ (loss of 0.83%). This illustrates the superiority of the Λ_2 scheme over the Λ_1 scheme, regardless of the time evolution of the vortex system.

Three runs were done: one without particle redistribution, one with Λ_2 redistribution at $t = 2$, and one with Λ_1 redistribution at $t = 2$. Contour plots for the first run are presented in Fig. 8.

The histograms of energy and enstrophy are provided in Fig. 9. Again, the energy decays due to LES diffusion. Due to vortex stretching, the enstrophy first increases. It then decreases due to vortex reconnection by viscous diffusion. As long as $\tilde{\omega}_\sigma$ remains close to ω_σ (here up to $t \approx 2$), the two curves, $\mathcal{E}$ and $\mathcal{E}_b$ remain identical. The Λ_1 scheme is again clearly unacceptable. The Λ_2 scheme performs much better. However, it is believed that it should have been used more often (i.e.,

FIGURE 8. Six rings interaction. 3-D contour plots of $\omega_\sigma = 2.0$ at $t = 0.0$, 2.0 and 4.0 .

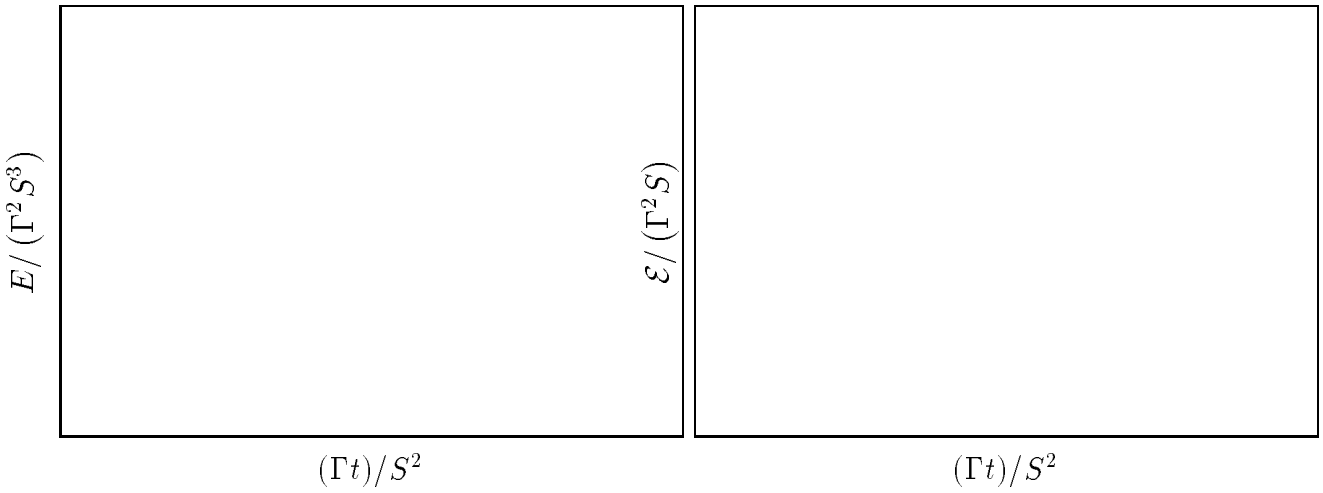

FIGURE 9. Six rings interaction. ——— : without redistribution: E and $\mathcal{E}$: • , $\mathcal{E}_b$: × ; ····· : with Λ_1 redistribution: E and $\mathcal{E}$: ▲ (inverted), $\mathcal{E}_b$: × ; – – – – : with Λ_2 redistribution: E and $\mathcal{E}$: ▲ , $\mathcal{E}_b$: × .

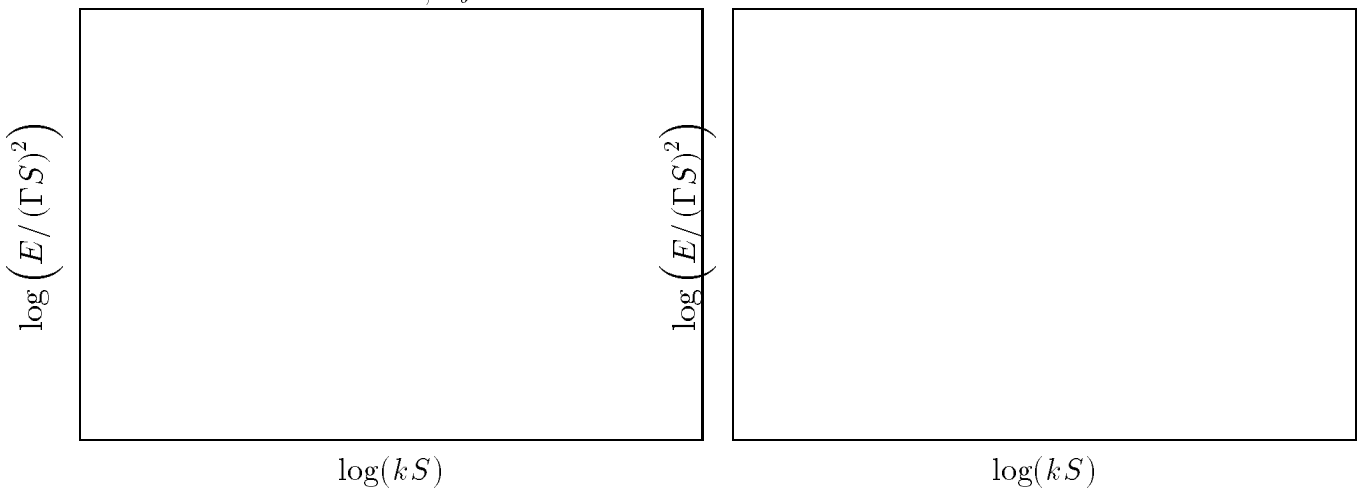

FIGURE 10. Six rings interaction. Energy spectrums: $t = 0$: ——— , $t = 1$: – – – – , $t = 2$: ····· , $t = 3$: —·— , $t = 4$: – – – ; k^8, k^6, k^4, k^{-1}, $k^{-5/3}$: ——— .

every 10 or 20 steps instead of every 80 steps) to give a better performance. Again, this could not be done, due to the $O(N^2)$ computational cost of the code. Finally, the correspondence $\tilde{\omega}_\sigma = \omega_\sigma$ (and hence $\mathcal{E} = \mathcal{E}_b$) is again better maintained with redistribution than without.

The energy spectrums are provided in Fig. 10. The high end of the spectrum starts filling up at $t \approx 2$. This is again indicative of problems with $\tilde{\omega}_\sigma \neq \omega_\sigma$ and is confirmed by a close look at both $\tilde{\omega}_\sigma$ and ω_σ for all particles. The low end of the spectrum remains well-behaved as time evolves, with very little spurious creation of linear impulse and of total vorticity. The six rings interaction here constitutes a "gentler" problem than the previous twelve rings interaction.

Again, regarding the "inertial" range of these vortex tubes interactions, it is again closer to a $(kS)^{-1}$ behavior (filtered by the Gaussian) than to a $(kS)^{-5/3}$

Kolmogorov behavior.

6.3 Six thin rings inviscid vortex system

To settle the issue, a run that replicates Kiya (1993) is also done. In that case, six circular rings of radius $R = 1$ and of circulation $\Gamma = 1$ are laid on the surface of the cube of size $S = 1.25$. Each ring is discretized using a single line of 256 particles (hence $h \approx 0.0245$. In Kiya, the high order algebraic smoothing is used, with $\sigma^\star = 0.10$. Recalling that the self-induced velocity of such a ring is obtained as (Leonard 1985, Winckelmans 1989)

$$U = \frac{\Gamma}{4\pi R}\left[\ln\left(\frac{8R}{\sigma^\star}\right) - \frac{1}{2}\right] \tag{31}$$

whereas the velocity of the ring with Gaussian smoothing is (Leonard 1985, Winckelmans 1989)

$$U = \frac{\Gamma}{4\pi R}\left[\ln\left(\frac{8R}{\sigma}\right) - 1.058\right] \ , \tag{32}$$

the proper scaling requires that our computation be done with $\sigma = 0.05724$. Thus, these are much thinner rings than before. Hence a wider "inertial" range is expected.

The computation is carried up to $t = 1.5$, with $\Delta t = 0.01$. Again, the symmetric scheme is used, $\alpha = 0.5$. This is also a simple VEM computation. Hence, no relaxation scheme, and no redistribution scheme. Finally, this is an inviscid computation. Hence, no LES.

The energy spectrums are provided in Fig. 11. As claimed by Kiya, the filtered spectrum, $E(kR)$ suggests a $(kR)^{-5/3}$ behavior. This is purely due to the filter, however. Indeed, from examining the unfiltered spectrums, $\hat{E}(kR)$, it is clear that (1) the behavior remains as $(kR)^{-1}$ for a long time (forever?), and (2) the computation eventually blows up (as was the case in Kiya). The histograms of energy and enstrophy are provided in Fig. 12. From the difference between the curves $\mathcal{E}$ and $\mathcal{E}_b$, it appears that the computation blows up at $t \approx 1.2$.

In conclusion, it appears that interactions involving only vortex tubes lead to a k^{-1} behavior. It may require the interaction between both vortex tubes and vortex sheets to obtain a Kolmogorov-like spectrum. A model involving spiral vortices (i.e., rolled-up vortex sheets) is presented in Lundgren (1982).

6.4 DNS of two rings fusion using the fast parallel tree code

This work was not done while at CTR. It was done in collaboration with Salmon, Warren and Leonard (Winckelmans *et al.* 1995d). It is also presented here in order to illustrate the capabilities of the fast parallel VEM code. We consider a high resolution DNS of the fusion of two vortex rings: radius $R = 1$, circulation $\Gamma = 1$, Gaussian vorticity distribution with $\sigma_R = 0.10$, spacing of the two rings center to center $S = 2.70$, angle of each ring w.r.t. vertical = 20 degs. Each ring is discretized with 126 sections and 225 particles per section (i.e., 7 layers, see Winckelmans & Leonard 1993). The inter-particle spacing is then $h \approx 0.05$. The computations were run with $\Delta t = 0.05$, $\sigma = 0.0625$, $\alpha = 0$, $\nu = 0.0025$ (i.e., $Re = \Gamma/\nu = 400$) on

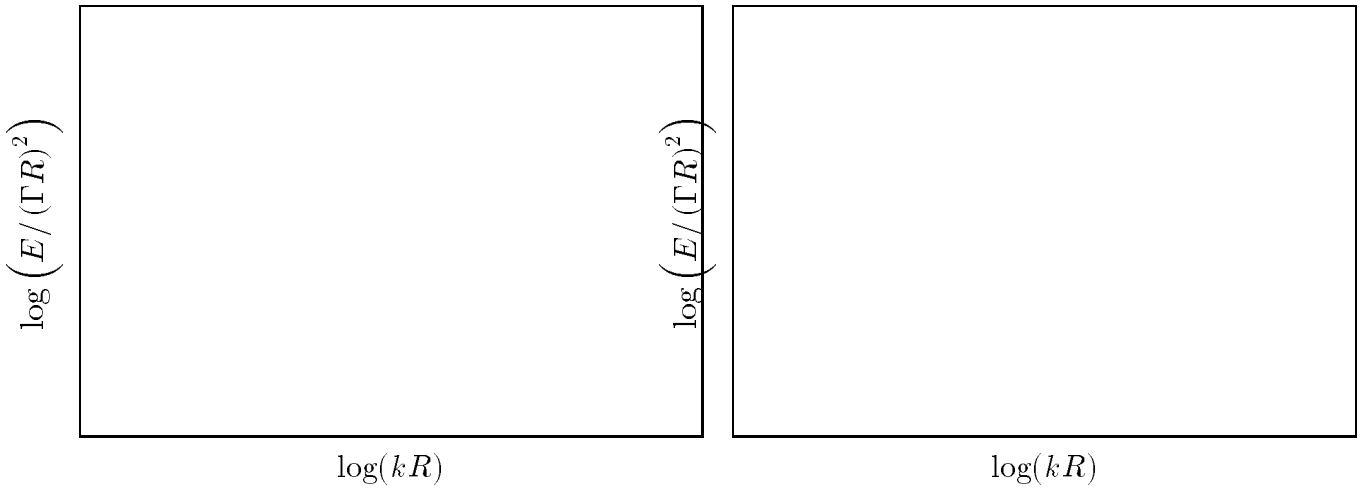

FIGURE 11. Six thin rings inviscid interaction. Filtered and unfiltered energy spectrums: $t = 0$: ——— , $t = 0.5$: - - - - , $t = 1$: ····· , $t = 1.5$: —·— ; k^8, k^{-1}, $k^{-5/3}$: ——— .

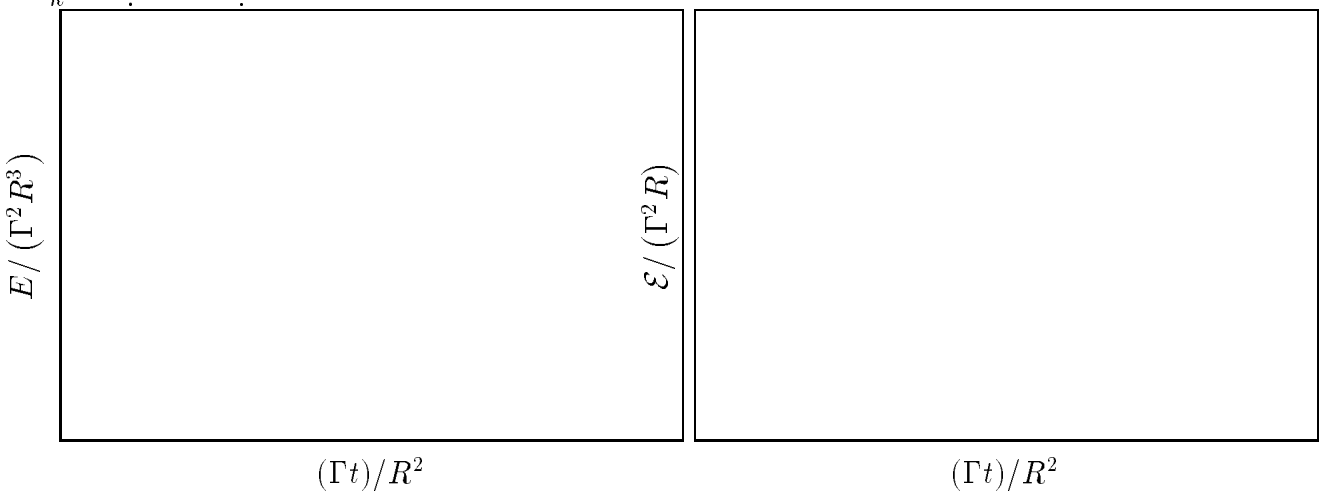

FIGURE 12. Six thin rings inviscid interaction. ——— : without redistribution: E and $\mathcal{E}$: • , $\mathcal{E}_b$: × .

both 32 nodes of the NAS IBM-SP2 and 64 nodes of the Caltech Intel Paragon. Initially, there were 56,700 particles (19 CPU secs per step on SP2-32 and 68 on Paragon-64). The Λ_2 particle redistribution scheme with $h = 0.05$ was used every 10 time steps. At the end of the run, there were 218,696 particles (87 CPU secs per step on SP2-32 and 236 on Paragon-64). The velocity error was roughly 0.0006 for the mean over all elements, and 0.0008 for the max.

It is seen in Fig. 13 that the diffusion scheme, when combined with the high order particle redistribution scheme, correctly captures the fusion process: First, the energy and enstrophy losses associated with the Λ_2 scheme are small enough that they cannot be seen in the histograms. (They can only slightly be seen when they are differentiated numerically.) Second, the normalized energy decay rate remains (almost) equal to the enstrophy, as it should. For comparison, a run without particle

FIGURE 13. Fusion of two vortex rings. 3-D view of the particle strengths at $t = 0.0, 5.4, 9.0$; Histogram of linear impulse, I_z, of energy, E, of enstrophy, $\mathcal{E}$, and of $-\frac{1}{\nu}\frac{dE}{dt}$.

redistribution was also done, see histograms in Fig. 13. In that case, the energy decay rate is clearly incorrect. Finally, the conservation of linear impulse is also much improved by the use of the redistribution scheme. Yet, even with particle redistribution, linear impulse starts decreasing at $t \approx 4$. It is believed that $\tilde{\omega}_\sigma$ is then beginning to deviate from ω_σ.

At this point, we are also experimenting with the two relaxation schemes when used in conjunction with the redistribution scheme. Results obtained so far are encouraging, yet too preliminary to be reported.

7. Conclusions

The VEM method has gone a long way since its early stages: accurate viscous diffusion, particle redistribution schemes, relaxation schemes for the particle vorticity field, fast and accurate field evaluation on both sequential and parallel platforms. This work is still in progress. The time has come to start developing LES models suitable to VEM. During this two-month visit at CTR, a dedicated $O(N^2)$ LES-VEM code was developed. Although slow, this code could be modified rapidly in order to experiment with many different schemes and ideas. Energy spectrums could also be computed. Some progress was accomplished in the following areas: (1) LES models and how to incorporate them into VEM, (2) energy spectrums and how to compute them, (3) particle redistribution schemes, (4) relaxation schemes. More work is needed, however, especially regarding (1) relaxation schemes and (2) further validation and development of LES models for VEM (which also requires that they eventually be incorporated into the fast parallel tree code.)

It is believed that, when combined with recent developments in vortex techniques for wall-bounded flows (Pépin 1990, Koumoutsakos 1993, Koumoutsakos & Leonard 1992, 1995, Koumoutsakos *et al.* 1994), a matured and well-developed methodology will permit the simulation of 3-D unsteady problems of engineering interest: flow past airfoils including vortex wake, and flow past bluff bodies including vortex wake. These body/wake computations will require the merging of the VEM code with a Boundary Element Method (BEM) in order to determine, at each time step, the vorticity flux required at solid boundaries in order to satisfy no-slip.

REFERENCES

Abramowitz, M. & Stegun, I. E. 1972 *Handbook of Mathematical Functions With Formulas, Graphs, and Mathematical Tables.* Applied Mathematics Series 55, Tenth Printing. National Bureau of Standards.

Brachet, M. E., Meneguzzi, M., Vincent, A., Politano, H. & Sulem, P. L. 1992 Numerical evidence of smooth self-similar dynamics and possibility of subsequent collapse for three-dimensional ideal flows. *Phys. Fluids A.* **4**(12), 2845–2854.

Degond, P. & Mas-Gallic, S. 1989 The weighted particle method for convection-diffusion equations, Part I: the case of an isotropic viscosity, Part II: the anisotropic case. *Math. Comput.* **53,** 485–526.

GERMANO, M., PIOMELLI, U., MOIN, P. & CABOT, W. 1991 A dynamic subgrid-scale eddy-viscosity model. *Phys. Fluids A.* **3**(7), 1760.

GHOSAL, S., LUND, T. S. & MOIN, P. 1992 A local dynamic model for large-eddy simulation. *Annu. Res. Briefs*, Center for Turbulence Research, Stanford Univ. & NASA Ames, 3–25.

GHOSAL, S. & MOIN, P. 1995 The basic equations for the large-eddy simulation of turbulent flows in complex geometry. *J. Comput. Phys.* **118,** 24–37.

GHOSAL, S., LUND, T. S., MOIN, P. & AKSELVOLL, K. A. 1995 A dynamic localization model for large-eddy simulation of turbulent flows. *J. Fluid Mech.* **286,** 229–255.

GOLUB, G. H. & VAN LOAN, C. F. 1983 *Matrix Computations.* John Hopkins Univ. Press.

KIYA, M. 1993 Simulating three-dimensional vortex motion by a vortex blob method. *Sādhanā.* **18(3,4),** 531–552.

KOUMOUTSAKOS, P. & LEONARD, A. 1992 Direct numerical simulations using vortex methods. *Proc. NATO Advanced Research Workshop: Vortex Flows and Related Numerical Methods*, Grenoble, France, 1992, 15–19.

KOUMOUTSAKOS, P. 1993 *Direct numerical simulations of unsteady separated flows using vortex methods.* Ph.D. thesis, California Institute of Technology.

KOUMOUTSAKOS, P., LEONARD, A. & PÉPIN, F. 1994 Viscous boundary conditions for vortex methods. *J. Comput. Phys.* **113**(1), 52–61.

KOUMOUTSAKOS, P. & LEONARD, A. 1995 High resolution simulations of the flow around an impulsively started cylinder using vortex methods. *J. Fluid Mech.* **296,** 1–38.

LEONARD, A. 1980 Review: Vortex methods for flow simulation. *J. Comput. Phys.* **37**(3), 289–335.

LEONARD, A. 1985 Computing three-dimensional incompressible flows with vortex elements. *Annu. Rev. Fluid Mech.* **17,** 523–559.

LESIEUR, M., COMTE, P. & MÉTAIS, O. 1995 Numerical simulations of coherent vortices in turbulence. *Applied Mechanics Rev.* **48**(3), 121–149.

LUNDGREN, T. S. 1982 Strained spiral vortex model for turbulent fine structure. *Phys. Fluids.* **25**(12), 2193–2203.

MANSOUR, N. N., FERZIGER, J. H. & REYNOLDS, W. C. 1978 *Large-eddy simulation of a turbulent mixing layer.* Report TF-11, Thermosciences Div., Dept. of Mech. Eng., Stanford University.

MAS-GALLIC, S. 1987 *Contribution à l'analyse numérique des méthodes particulaires.* Thèse d'Etat, Université Paris VI.

MOIN, P. & JIMINEZ, J. 1993 Large eddy simulation of complex turbulent flows. *AIAA 24th Fluid Dynamics Conference*, Orlando, Fl., AIAA paper 93-3099.

MOIN, P., CARATI, D., LUND, T., GHOSAL, S, & AKSELVOLL, K. 1994 Developments and applications of dynamic models for large eddy simulation of complex flows. *74th Fluid Dynamics Symposium on Application of Direct and Large Eddy Simulation to Transition and Turbulence*, Chania, Crete, Greece, AGARD-CP-551, 1-1–9.

PEDRIZZETTI, G. 1992 Insight into singular vortex flows. *Fluid Dyn. Res.* **10,** 101-115.

PÉPIN, F. 1990 *Simulation of flow past an impulsively started cylinder using a discrete vortex method.* Ph.D. thesis, California Institute of Technology.

PHILLIPS, O. M. 1956 The final period of decay of non-homogeneous turbulence. *Proc. Cambridge Phil. Soc.* **52**(1), 135–151.

ROGALLO R. S. & MOIN, P. 1984 Numerical simulation of turbulent flows. *Annu. Rev. Fluid Mech.* **16,** 99–137.

SAFFMAN, P. G. & MEIRON, D. I. 1986 Difficulties with three-dimensional weak solutions for inviscid incompressible flow. *Phys. Fluids.* **29**(8), 2373–2375.

SALMON, J. K. 1990 *Parallel hierarchical N-body methods.* Ph.D. thesis, California Institute of Technology.

SALMON, J. K. & WARREN, M. S. 1994 Skeletons from the treecode closet. *J. Comput. Phys.* **111**(1), 136–155.

SALMON, J. K., WARREN, M. S. & WINCKELMANS, G. S. 1994 Fast parallel tree codes for gravitational and fluid dynamical N-body problems. *Int. J. Supercomputer Applications.* **8**(2), 129–142.

SHARIFF, K., LEONARD, A. & FERZIGER, J. H. 1989 *Dynamics of a class of vortex rings.* NASA Technical Memorandum 102257, Ames Research Center.

WARREN, M. S. & SALMON, J. K. 1995 A Parallel, Portable and Versatile Treecode. *Proc. Seventh SIAM Conference on Parallel Processing for Scientific Computing*, San Francisco, CA, 15–17 Feb., 1995, 319–324.

WINCKELMANS, G. S. & LEONARD, A. 1988 Weak solutions of the three-dimensional vorticity equation with vortex singularities. *Phys. Fluids, Letters.* **31**(7), 1838–1839.

WINCKELMANS, G. S. & LEONARD, A. 1989 Improved vortex methods for three-dimensional flows. *SIAM Workshop on Mathematical Aspects of Vortex Dynamics*, Leesburg, VA, April, 1988, *SIAM Proc. Series*, R. E. Caflisch ed., 25–35.

WINCKELMANS, G. S. 1989 *Topics in vortex methods for the computation of three- and two-dimensional incompressible unsteady flows.* Ph.D. thesis, California Institute of Technology.

WINCKELMANS, G. S. 1993 Comments on a paper by Kiya et al. on the numerical simulation of pseudo-elliptical vortex rings using the vortex particle method. *Fluid Dyn. Res., Brief Comm.* **12,** 57–60.

WINCKELMANS, G. S. & LEONARD, A. 1993 Contributions to vortex particle methods for the computation of three-dimensional incompressible unsteady flows. *J. Comput. Phys.* **109**(2), 247–273.

WINCKELMANS, G. S., SALMON, J. K., WARREN, M. S. & LEONARD, A. 1995 The fast solution of three-dimensional fluid dynamical N-body problems using parallel tree codes: vortex element method and boundary element method. *Proc. Seventh SIAM Conference on Parallel Processing for Scientific Computing*, San Francisco, CA, 15–17 Feb., 1995, 301–306.

WINCKELMANS, G. S., SALMON, J. K., LEONARD, A. & WARREN, M. S. 1995 Three-dimensional vortex particle and panel methods: Fast tree-code solvers with active error control for arbitrary distributions/geometries. *Proc. Forum on Vortex Methods for Engineering Applications*, Albuquerque, NM, 22–24 Feb., 1995, 25-43.

WINCKELMANS, G. S., SALMON, J. K., LEONARD, A. & WARREN, M. S. 1995 Simulations of airfoil three-dimensional vortex wakes via fast vortex particle parallel and sequential tree codes. In *Proc. Third Annual Conference of the CFD Society of Canada*, Banff, Alberta, 25–27 June, 1995, 349–356.

WINCKELMANS, G. S., SALMON, J. K., WARREN, M. S., LEONARD, A. & JODOIN, B. Application of fast parallel and sequential tree codes to computing three-dimensional flows with the vortex element and boundary element methods. To appear in *Proc. Second International Workshop on Vortex Flows and Related Numerical Methods*, Montréal, Canada, 20–24 August, 1995 (submitted Sept. 95).